

Investigating flavour-dependent chiral magnetic effect with a multiphase transport model

Ling Huang,¹ Chun-Wang Ma,^{1,*} and Guo-Liang Ma^{2,†}

¹*Institute of Particle and Nuclear Physics,
Henan Normal University, Xinxiang 453007, China*

²*Shanghai Institute of Applied Physics,
Chinese Academy of Sciences, Shanghai 201800, China*

Abstract

Because the properties of the QCD phase transition and Chiral Magnetic Effect (CME) depend on the number of quark flavours (N_f) and quark mass, relativistic heavy-ion collisions provide a natural environment to investigate the flavour features due to the occurring of quark deconfinement. We introduce an initial two-flavour and three-flavour dipole charge separation into a multiphase transport (AMPT) model to investigate the flavour dependence of the CME. By taking advantage of the recent ALICE data of charge azimuthal correlations with identified hadrons, we attempt to disentangle two-flavour and three-flavour CME scenarios in Pb+Pb collisions at 2.76 TeV. We find that the experimental data show a certain potential to distinguish the two cases, therefore we further suggest to collect more data to clarify the possible flavour dependence in the future experiment.

PACS numbers:

*machunwang@126.com

†glma@sinap.ac.cn

I. INTRODUCTION

Relativistic heavy-ion collisions serve as a very good laboratory to investigate the intrinsic characters of fundamental QCD interactions, because it can convert a confined hadronic matter with chiral symmetry breaking into a deconfined partonic matter with chiral symmetry restoration by varying temperature and baryon chemical potential [1–3]. In the past decade, plenty of experimental results announce that a strongly-coupling Quark Gluon Plasma (sQGP) has been created by relativistic heavy-ion collisions at the Relativistic Heavy-Ion Collider (RHIC) and the Large Hadron Collider (LHC) [4–6]. As the same time, an extremely large magnetic field can be produced in the early state of relativistic heavy-ion collisions due to the fast relative motion of two positive-charged nuclei [7, 8]. If there occurs any topology-changing transitions which result in a chirality asymmetry between left- and right-handed quarks in the early state of heavy-ion collisions, a electric current will be generated along the magnetic field direction, which is so-called Chiral Magnetic Effect [9]. The experimental measurements of charge azimuthal correlation ($\gamma = \langle \cos(\Psi_\alpha + \Psi_\beta - 2\Psi_{RP}) \rangle = \langle \cos(\Psi_\alpha + \Psi_\beta - 2\phi_c) \rangle / v_{2,c}$) show some consistent results with the CME expectation [10–12], though the truth is still on debate because many important background sources can largely contribute to the signal [13–19]. But the scientific importance of the CME is undoubted, since the CME is deeply linked to the two intrinsic properties of strong interaction, i.e. chiral symmetry and confinement. In other words, if the CME exists in relativistic heavy-ion collisions, it will be a strong evidence of deconfinement and chiral symmetry restoration in a hot and dense strong-interacting system [20].

Lattice QCD calculations reveal that the properties of the QCD phase transition depend on the number of quark flavours (N_f) and their masses [1, 2]. The critical temperatures for deconfinement (or chiral symmetry restoration) are different between 2-flavour ($N_f=2$) QCD and 3-flavour ($N_f=3$) QCD. It is even argued that there could be a flavour hierarchy in the deconfinement transition of QCD matter [21]. From the QCD phase diagram of 3-flavour QCD, it sheds light on the fact that the order of phase transition strongly depends on light quark (u,d) masses and a strange (s) quark mass [1, 2]. At the same time, the equation of state of QCD matter must has dependences on the number of quark flavours (N_f) and their masses [1, 3]. On the other hand, the CME also carries the information about the number of quark flavours (N_f), because the CME current is proportional to a trace coefficient related

to anomalous triangle diagram which gives a coefficient of $5/9$ to the 2-flavour CME but $2/3$ for the 3-flavour CME [22]. It results in a relative CME current difference of $1/6$ between 2-flavour and 3-flavour cases. However, because the traditional experimental observable γ of charge azimuthal correlation include all inclusive charged hadrons, it limits ones to measure the relative difference. Recently, the ALICE collaboration measured the identified hadron triggered charge azimuthal correlation, e.g. kaon-hadron correlation, which enable us to access the flavour property of the CME [23]. Another advantage of kaon-hadron correlation is that it can avoid the contamination from ρ meson decay, which presumably play a significant influence on the CME observable [24]. In this work, we implement a multiphase transport (AMPT) model to investigate the flavour dependence of the CME. In our previous work, we imported the initial CME-like dipole charge separation to the AMPT model with a constant separation percentage, and found that though the original AMPT model can reproduce 60-70% magnitude of the CME observable γ in Au+Au collisions at 200 GeV, an initial charge separation percentage of $\sim 10\%$ is needed to closely match the STAR data, and demonstrate that final state interactions strongly suppress the initial CME effect [25]. In this work, we will improve our method to study the γ correlators in Pb+Pb collisions at 2.76 TeV, by taking two following improvements into account. Firstly, we use a centrality-dependent charge separation percentage which is assumed to be proportional to the magnitude of magnetic field in Pb+Pb collisions, which is more reasonable for simulating the CME. Secondly, we consider both 2-flavour and 3-flavour cases for the initial charge separation to mimic the 2-flavour and 3-flavour CME effect, while we only considered two flavours of quarks (u and d) in our previous work [25].

This paper is organized as follows. We give a short introduction of our model and the method to introduce the 2-flavour and 3-flavour dipole charge separations in Sec. II. In Sec. III, we present our simulation results and expand some discussions. Finally, we summarize in Sec. IV.

II. THE AMPT MODEL

We implemented the AMPT model with string meting mechanism in this study [26]. The AMPT model, which is a Monte Carlo hybrid transport model, includes four main stages of Relativistic heavy-ion collisions, i.e initial condition, parton cascade, hadronization,

and hadronic rescatterings. The initial condition, which includes the spatial and momentum distributions of minijet partons and soft string excitations, is obtained from HIJING model [27, 28], where minijets and soft string excitations are fragmented into hadrons according to the Lund string fragmentation [29]. The string melting mechanism can convert all hadrons to quarks according to the flavour and spin structures of their valence quarks, which mimic the QCD deconfinement that results in a formation of a quark and anti-quark plasma. Next the plasma starts the parton evolution which is simulated by Zhang's parton cascade (ZPC) model [30], where the perturbative QCD partonic cross section is controlled by the strong coupling constant and Debye screening mass. For hadronization, the model recombines the freezeout partons to hadrons through a naive coalescence model. The evolutions of the subsequent hadronic phase is then described by a relativistic transport (ART) model [31]. Recently, Ma and Lin found the string melting AMPT model with an universal setting of tuned parameters can reasonably reproduce dN/dy , p_T -spectra, azimuthal anisotropies v_n , and longitudinal decorrelation in A+A collisions at both RHIC and LHC energies [32]. Therefore, we take the same setting of parameters in this work. However, because some hadronic reaction channels from the ART part does not conserve electric charge, we turn off the hadron evolution but only keep resonance decays to ensure charge conservation event-by-event-ly to study the charge-dependent CME-related observables.

To study the CME current, we need to introduce an initial charge separation into the initial condition of the AMPT model, since the motion of charges are not directionally separated but isotropic in the original version of AMPT model. In order to separate a percentage of the initial charges, we use the same method invented by Ma and Zhang in Ref. [25]. For a given flavour of quarks, let us say u quark, we switch a percentage of the downward moving u quarks with those of the upward moving \bar{u} quarks in such a way that the total momentum is conserved, and likewise for \bar{d} and d quarks and \bar{s} and s quarks. The percentage f can be defined as,

$$f = \frac{N_{\uparrow(\downarrow)}^{+(-)} - N_{\downarrow(\uparrow)}^{+(-)}}{N_{\uparrow(\downarrow)}^{+(-)} + N_{\downarrow(\uparrow)}^{+(-)}} \propto B_y, \quad (1)$$

where N is the number of quarks, + and - denote positive-charged and negative-charged, and \uparrow and \downarrow represents upward and downward for momentum, where we assume that magnetic field is in the y direction. We can introduce 2-flavour and 3-flavour CME-like electric currents by with and without including the separation of strange quarks. For all cases, we assume

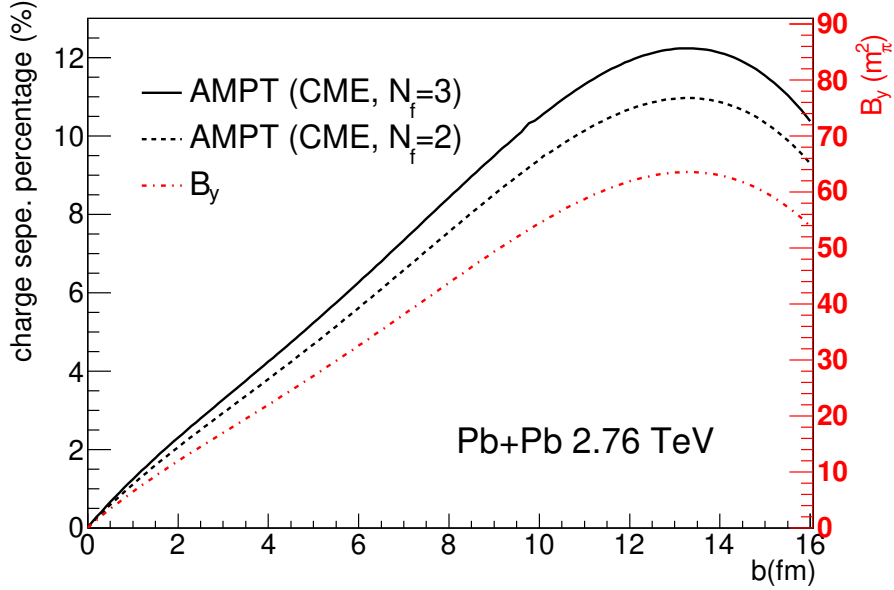


FIG. 1: (Color online) The impact parameter b dependences of magnetic field B_y (dot-dash, right y axis) and initial charge separation percentages for 2-flavour CME (dash) and 3-flavour CME (solid) in Pb+Pb collisions at 2.76 TeV. The magnetic field B_y is taken from Ref. [8].

that all kinds of flavours of quarks share a same value of charge separation percentage for simplicity. In principle, the charge separation percentage should be presumably proportional to the magnetic field B_y . Since the magnitude of magnetic field is impact parameter b -dependent, the percentage f should depend on b or centrality bin. To obtain the b -dependent percentage, we take the centrality dependence of magnetic field B_y in Pb+Pb collisions at 2.76 TeV from Ref. [8], which is presented by red dot-dash curve in Figure 1. By assuming that the initial charge percentage obeys Eq. (1), we use the AMPT model with the initial charge separation to fit the charge azimuthal correlation γ from the ALICE data [12] to get the corresponding proportional coefficient for two CME scenarios. Thus, we obtain b -dependent initial charge separation percentages, as shown by dash ($N_f=2$) and solid ($N_f=3$) curves in Figure 1, which serve as our input for simulating the CME-related observables with the AMPT model.

III. RESULTS AND DISCUSSIONS

For Pb+Pb collisions at 2.76 TeV, we calculate two kinds of charge azimuthal correlations, one case is the traditional observable, which is usually called as the charge azimuthal correlation γ , where two particles belongs to unidentified charged hadrons. The other case is that identified hadron triggered $c_{\alpha\beta}^{ij}$ correlator, where one of two particles is identified hadron, e.g. kaon. We will show the two cases in the two following subsections, respectively.

A. Charge azimuthal correlation γ

We calculate the traditional CME observable γ through a similar method to what the experimentalists did [10–12, 33]. The charge azimuthal correlation (correlator) γ is defined as,

$$\gamma = \cos(\varphi_\alpha + \varphi_\beta - 2\Psi_{RP}) \quad (2)$$

φ_α and φ_β represent two charged particles' azimuthal angles, α and β denotes their charge which can be "+" or "-", and Ψ_{RP} is the reaction plane angle.

The reaction plane angle Ψ_{RP} is represented by the second order of participant plane Ψ_2 in our calculations,

$$\Psi_n = \frac{1}{n} \left[\arctan \frac{\langle r^n \sin(n\varphi) \rangle}{\langle r^n \cos(n\varphi) \rangle} + \pi \right] \quad (3)$$

, which can be calculated based on the initial geometry information of partonic system from the AMPT model, where r is the displacement of the participating partons from the center of mass, ϕ is the azimuthal angle of the participating partons in the transverse plane, and we take $n=2$ [34, 35].

By applying the initial charge separation function into AMPT model, we get the results of γ correlator for different cases. In Figure 2, square symbol represents experimental data from ALICE [12], while circle symbol represents the original AMPT results without initial charge separation. We can see that the original AMPT model can basically describe the experimental data for the centrality bin of 0-30%, but its magnitude is smaller than the experimental data for the centrality bin of 30%-70%, especially for opposite-charge data. This indicates the original AMPT model can serve as a good background model to study the CME, since it can give a main part of observable even without introducing any initial charge separation. This is mainly because of the advantage of the AMPT model that it

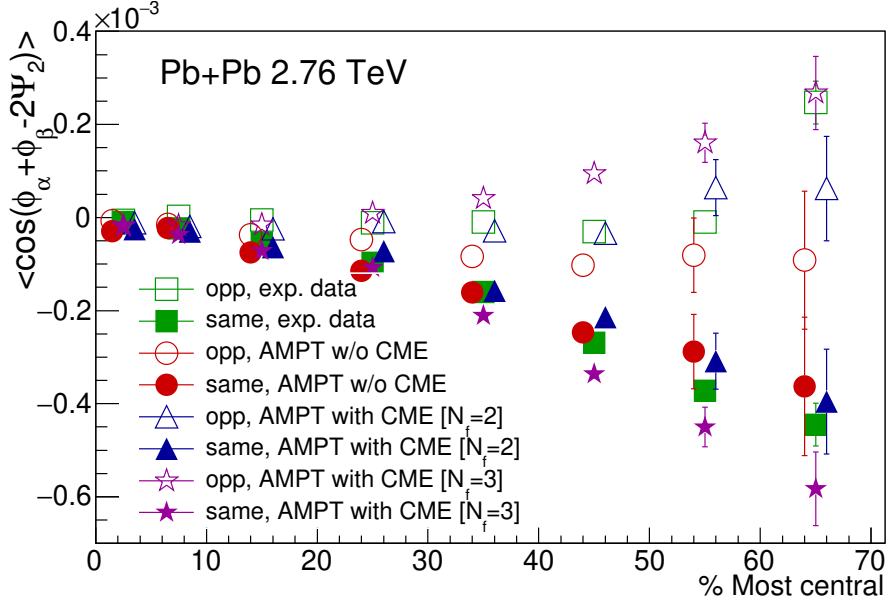


FIG. 2: (Color online) The centrality dependence of charge-particle azimuthal correlation γ from Pb+Pb collisions at 2.76 TeV, where the experimental data are taken from Ref. [12].

includes several important background sources, transverse momentum conservation [16, 36] and local charge conservation [36], etc. The triangle symbol represents the results from the AMPT model with initial 2-flavour charge separation for u and d quarks. For the centrality bin of 0-60%, the AMPT results is similar to the experimental data. But for the centrality bin of 60%-70%, it can reproduce same-charge correlation but underestimate opposite-charge one. On the other hand, the star symbol represents the AMPT results with initial 3-flavour charge separation for u,d and s quarks. We can see that the results from the 3-flavour case is close to the experimental data for the centrality bin of 0-30%. Unfortunately, it overestimate experimental data for the both opposite- and same-charge correlations for the centrality bin of 30%-70%. In general, all of three cases can describe the experimental data qualitatively, but none of them can perfectly describe both opposite- and same-charge experimental data for all centrality bins.

B. Identified hadron triggered charge azimuthal correlation $c_{\alpha\beta}^{ij}$

To see the difference between 2-flavour CME and 3-flavour CME, it is the key to see if the strange quark participant the CME process. Therefore, it will be very helpful to see the

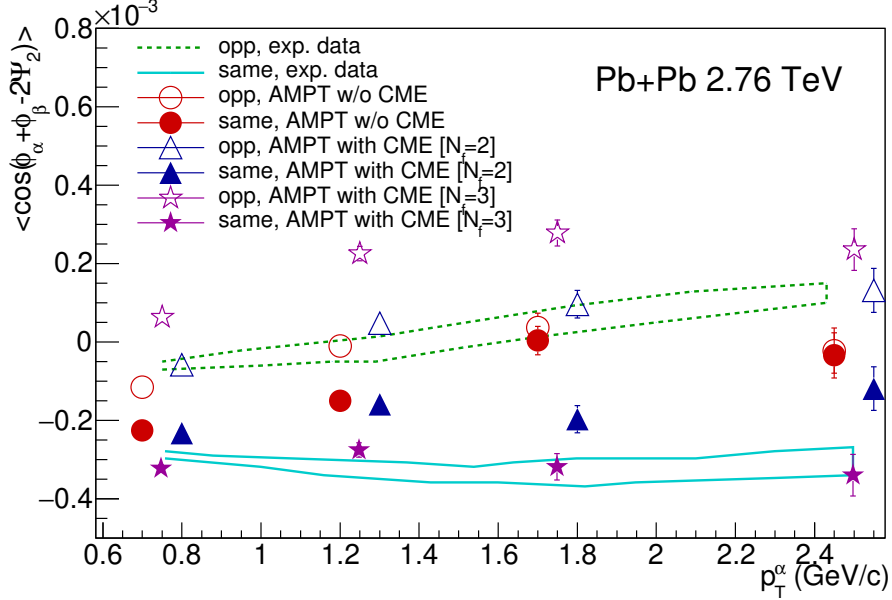


FIG. 3: (Color online) The p_T dependences of hadron-hadron charge azimuthal correlations in Pb+Pb collisions at 2.76 TeV (30-50%), where two bands represent the ALICE data [23].

charge azimuthal correlation with a identified hadron as a trigger particle, especially when a charged kaon is the triggered hadron since it consists of a strange quark. We defined the identified hadron triggered charge azimuthal correlation in a same way as what the ALICE collaboration did [23],

$$c_{\alpha\beta}^{ij}(p_T) = \langle \cos(\varphi_\alpha^i(p_T) + \varphi_\beta^j - 2\Psi_{RP}) \rangle, \quad (4)$$

where i denotes an identified hadron and j denotes an unidentified or inclusive charged hadron, α and β denotes their charges which can be "+" or "-", and Ψ_{RP} is the reaction plane angle for which we still use Ψ_2 to represent it. The observable is studied as a function of p_T , which is the transverse momentum of the identified hadron.

To see the difference between 2-flavour CME and 3-flavour CME, we calculated both hadron-hadron and kaon-hadron correlations. Figure 3 present the p_T dependences of hadron-hadron charge azimuthal correlations in Pb+Pb collisions at 2.76 TeV (30-50%), where the experimental data are shown by two bands. We can see the original AMPT results without initial charge separation (circles) can reproduce the experimental opposite-charge data, but fails for describing the same-charge data. The AMPT result with initial 2-flavour charge separation (triangles) also can describe the opposite-charge data, but underestimate the magnitudes of same-charge data. The AMPT results with initial 3-flavour

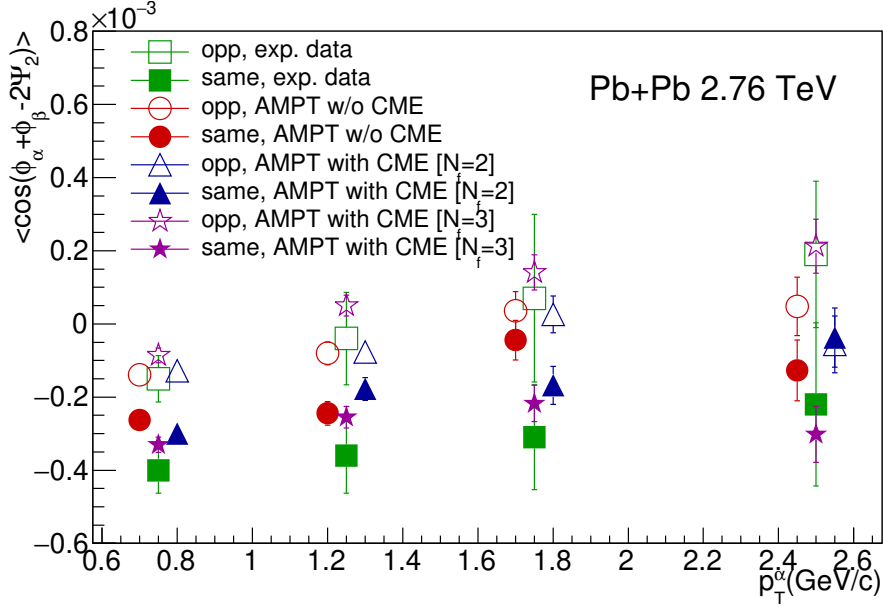


FIG. 4: (Color online) Same as Figure 3 but for kaon-hadron charge azimuthal correlations.

charge separation can describe the opposite-charge data, but overestimate the same-charge data. Therefore, neither 2-flavour case nor 3-flavour case can well reproduce the experimental data.

We next study kaon-hadron charge azimuthal correlation, because it may reflect some sensitive information about the flavour dependence of the CME without any influence from ρ meson decays. Figure 4 shows the p_T dependences of kaon-hadron charge azimuthal correlations in Pb+Pb collisions at 2.76 TeV (30-50%), where squares represent the new ALICE data. It seems that the original AMPT results without initial charge separation (circles) can only describe experimental opposite-charge data, but overestimate the same-charge data. It looks that both 2-flavour case and 3-flavour case can describe the experimental data if considering the large experimental errors. However, it is difficult to judge which of the two CME cases is better for the moment. On the other hand, since the difference between 2-flavour and 3-flavour results is limited, it will be helpful to have more event statistics to disentangle two scenarios of CME clearly in the future experiments.

IV. SUMMARY

We introduce a centrality-dependent initial 2-flavour and 3-flavour charge separation into the AMPT model which is a very good background/baseline model to study the CME. We found that both kinds of CME can improve the descriptions to the traditional CME observable of charge azimuthal correlation γ . We compare the AMPT results with the new ALICE measurement of the charge azimuthal correlations with identified hadrons (i.e. hadron-hadron correlation vs. kaon-hadron correlation). We found that the charge azimuthal correlation with identified hadrons, especially with identified kaons, has a potential to disentangle 2-flavour CME from 3-flavour CME. However, within the current experimental uncertainties, it is difficult to say which-flavour CME the ALICE data favour. Therefore, more statistics are required to verify it clearly in the future experiments, which would help us to further understand more aspects of the QCD phase transitions.

ACKNOWLEDGMENTS

This work is supported by the Major State Basic Research Development Program in China under Grant No. 2014CB845404, the National Natural Science Foundation of China under Grants No. 11522547, 11375251, and 11421505 and the Program for the Excellent Youth at Henan Normal University under Grant No. 154100510007.

-
- [1] F. Karsch, Lect. Notes Phys. **583**, 209 (2002) [hep-lat/0106019].
 - [2] H. T. Ding, F. Karsch and S. Mukherjee, Int. J. Mod. Phys. E **24**, no. 10, 1530007 (2015) [arXiv:1504.05274 [hep-lat]].
 - [3] A. Bazavov *et al.* [HotQCD Collaboration], Phys. Rev. D **90**, 094503 (2014) [arXiv:1407.6387 [hep-lat]].
 - [4] J. Adams *et al.* [STAR Collaboration], Nucl. Phys. A **757**, 102 (2005) [nucl-ex/0501009].
 - [5] K. Adcox *et al.* [PHENIX Collaboration], Nucl. Phys. A **757**, 184 (2005) [nucl-ex/0410003].
 - [6] K. Aamodt *et al.* [ALICE Collaboration], JINST **3**, S08002 (2008).
 - [7] A. Bzdak and V. Skokov, Phys. Lett. B **710** 171 (2012) [arXiv:1111.1949 [hep-ph]].
 - [8] W. T. Deng and X. G. Huang, Phys. Rev. C **85**, 044907 (2012) [arXiv:1201.5108 [nucl-th]].

- [9] K. Fukushima, D. E. Kharzeev and H. J. Warringa, Phys. Rev. D **78**, 074033 (2008) [arXiv:0808.3382 [hep-ph]].
- [10] B. I. Abelev *et al.* [STAR Collaboration], Phys. Rev. Lett. **103**, 251601 (2009) [arXiv:0909.1739 [nucl-ex]].
- [11] B. I. Abelev *et al.* [STAR Collaboration], Phys. Rev. C **81**, 054908 (2010) [arXiv:0909.1717 [nucl-ex]].
- [12] B. Abelev *et al.* [ALICE Collaboration], Phys. Rev. Lett. **110**, no. 1, 012301 (2013) [arXiv:1207.0900 [nucl-ex]].
- [13] S. Schlichting and S. Pratt, Phys. Rev. C **83**, 014913 (2011) [arXiv:1009.4283 [nucl-th]].
- [14] S. Pratt, S. Schlichting and S. Gavin, Phys. Rev. C **84**, 024909 (2011) [arXiv:1011.6053 [nucl-th]].
- [15] A. Bzdak, V. Koch and J. Liao, Phys. Rev. C **81**, 031901 (2010) [arXiv:0912.5050 [nucl-th]].
- [16] A. Bzdak, V. Koch and J. Liao, Phys. Rev. C **83**, 014905 (2011) [arXiv:1008.4919 [nucl-th]].
- [17] J. Liao, V. Koch and A. Bzdak, Phys. Rev. C **82**, 054902 (2010) [arXiv:1005.5380 [nucl-th]].
- [18] F. Wang, Phys. Rev. C **81**, 064902 (2010) [arXiv:0911.1482 [nucl-ex]].
- [19] A. Bzdak, V. Koch and J. Liao, Lect. Notes Phys. **871**, 503 (2013) [arXiv:1207.7327 [nucl-th]].
- [20] D. E. Kharzeev, L. D. McLerran and H. J. Warringa, Nucl. Phys. A **803**, 227 (2008) [arXiv:0711.0950 [hep-ph]].
- [21] R. Bellwied, S. Borsanyi, Z. Fodor, S. D. Katz and C. Ratti, Phys. Rev. Lett. **111**, 202302 (2013) [arXiv:1305.6297 [hep-lat]].
- [22] D. E. Kharzeev and D. T. Son, Phys. Rev. Lett. **106**, 062301 (2011) [arXiv:1010.0038 [hep-ph]].
- [23] J. Onderwaater [ALICE Collaboration], J. Phys. Conf. Ser. **612**, no. 1, 012044 (2015).
- [24] J. Zhao, H. Li and F. Wang, arXiv:1705.05410 [nucl-ex].
- [25] G. L. Ma and B. Zhang, Phys. Lett. B **700**, 39 (2011) [arXiv:1101.1701 [nucl-th]].
- [26] Z. W. Lin, C. M. Ko, B. A. Li, B. Zhang and S. Pal, Phys. Rev. C **72**, 064901 (2005) [nucl-th/0411110].
- [27] X. N. Wang and M. Gyulassy, Phys. Rev. D **44**, 3501 (1991).
- [28] M. Gyulassy and X. N. Wang, Comput. Phys. Commun. **83**, 307 (1994) [nucl-th/9502021].
- [29] T. Sjostrand, P. Eden, C. Friberg, L. Lonnblad, G. Miu, S. Mrenna and E. Norrbin, Comput. Phys. Commun. **135**, 238 (2001) [hep-ph/0010017].
- [30] B. Zhang, Comput. Phys. Commun. **109**, 193 (1998) [nucl-th/9709009].

- [31] B. A. Li and C. M. Ko, Phys. Rev. C **52**, 2037 (1995) [nucl-th/9505016].
- [32] G. L. Ma and Z. W. Lin, Phys. Rev. C **93**, no. 5, 054911 (2016) [arXiv:1601.08160 [nucl-th]].
- [33] S. A. Voloshin, Phys. Rev. C **70**, 057901 (2004) [hep-ph/0406311].
- [34] B. Alver and G. Roland, Phys. Rev. C **81**, 054905 (2010) Erratum: [Phys. Rev. C **82**, 039903 (2010)] [arXiv:1003.0194 [nucl-th]].
- [35] G. L. Ma and X. N. Wang, Phys. Rev. Lett. **106**, 162301 (2011) [arXiv:1011.5249 [nucl-th]].
- [36] S. Pratt, arXiv:1002.1758 [nucl-th].